Journal of Coordination Chemistry

ISSN: 0095-8972 (Print) 1029-0389 (Online) Journal homepage: http://www.tandfonline.com/loi/gcoo20

A cobalt(II) complex with anionic and neutral N-donor ligands: synthesis, crystal structure, and application as a heterogeneous catalyst for olefin epoxidation with tert-BuOOH

Leila Tabrizi, Hossein Chiniforoshan & Patrick Mcardle

To cite this article: Leila Tabrizi, Hossein Chiniforoshan & Patrick Mcardle (2015) A cobalt(II) complex with anionic and neutral N-donor ligands: synthesis, crystal structure, and application as a heterogeneous catalyst for olefin epoxidation with tert-BuOOH, Journal of Coordination Chemistry, 68:6, 980-992, DOI: 10.1080/00958972.2015.1007964

To link to this article: http://dx.doi.org/10.1080/00958972.2015.1007964

Journal of Coordination Chemistry, 2015
Vol. 68, No. 6, 980–992, http://dx.doi.org/10.1080/00958972.2015.1007964

A cobalt(II) complex with anionic and neutral N-donor ligands: synthesis, crystal structure, and application as a heterogeneous catalyst for olefin epoxidation with *tert*-BuOOH

LEILA TABRIZI†, HOSSEIN CHINIFOROSHAN†* and PATRICK MCARDLE‡

†Department of Chemistry, Isfahan University of Technology, Isfahan, Iran
‡School of Chemistry, National University of Ireland Galway, Galway, Ireland

(*Received 31 August 2014; accepted 30 December 2014*)

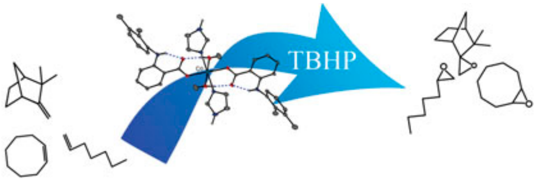

A cobalt(II) complex containing deprotonated mefenamic acid (Hmef) and imidazole (HIm), [Co(mef)$_2$(HIm)$_2$(CH$_3$OH)$_2$], has been synthesized and characterized by spectroscopic techniques (UV–vis, IR, and EPR), elemental analysis, and single-crystal X-ray diffraction analysis. The structure has distorted octahedral geometry around cobalt. The mefenamate is a monodentate ligand coordinated to the Co(II) through a carboxylate oxygen. This complex was tested as a catalyst for epoxidation of alkenes with *tert*-BuOOH in 1,2-dichloroethane solution. This catalyst was effective in epoxidation of various alkenes including non-activated terminal alkenes. The effects of solvent, oxidant, and temperature on the epoxidation of cyclohexene were investigated. In all cases, high yields of epoxidized alkenes were obtained.

Keywords: Heterogeneous catalysis; *tert*-BuOOH; Mefenamic acid; Epoxidation; Cobalt(II)

1. Introduction

Epoxides are useful starting materials for value added products such as pharmaceuticals and flavor and fragrance molecules [1–4]. In addition, they can be used in polymer production, acting as precursors for complex molecules due to the strained oxirane ring [5], providing detergents, surfactants, antistatic agents, corrosion protection agents, textiles, lubricating oils, and cosmetics [6]. So, there is continuing interest in the development of efficient and selective methods for preparation of epoxides.

---

*Corresponding author. Email: Chinif@cc.iut.ac.ir

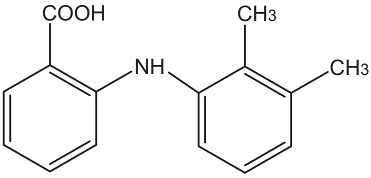

Scheme 1. Mefenamic acid structure.

The use of transition-metal complexes as catalysts for epoxidation has led to a variety of catalytic systems [7–13].

Cobalt complexes are among the most widely employed catalysts for the oxidation of organic substrates. Despite extensive use in industrial oxidations, little is known about the catalytically active cobalt species [14–18]. Cobalt(II) Schiff base complexes [19–24] and cobalt(II) and cobalt(III) complexes [25–29], cobalt-containing polyoxotungstate [30], and $Co(thd)_2$ (thd = bis(2,2,6,6-tetramethyl-3,5-heptanedionato)) [31] are all effective epoxidation catalysts. Cobalt(III)-peroxo/alkylperoxo species are regarded as intermediates in these catalytic processes [32, 33].

Cobalt catalysis of olefin oxidation requires a ligand that is sufficiently robust to withstand oxidative conditions. Among the various possibilities, we chose mefenamic acid for this study of olefin oxidation. Some complexes of mefenamic acid with interesting applications have been reported [34–36]. In the present work, we report the synthesis and crystal structure of a Co(II)-complex containing mefenamic acid (Hmef), scheme 1, and imidazole (HIm) ligands $[Co(mef)_2(HIm)_2(CH_3OH)_2]$ (**1**). In addition, its catalytic performance in epoxidation of various olefins was investigated. The effects of different solvents, oxidants, and temperature on the activity and selectivity of the catalyst were also investigated.

2. Experimental

2.1. *Materials*

All chemicals and solvents were purchased from Merck or Sigma-Aldrich and used without purification. Mefenamic acid was obtained from the Raha Pharmaceutical Company.

2.2. *Physical measurements*

Fourier transform infrared spectra were recorded on an FT-IR JASCO 680-PLUS spectrometer from 4000 to 400 cm^{-1} using KBr pellets. Elemental analyses were performed by using a Leco, CHNS-932 elemental analyzer. Molar conductivity measurements were carried out with a Crison Basic 30 conductometer. Ultraviolet–visible (UV–vis) spectra were measured with a Lambda 25 spectrophotometer. Gas chromatography experiments (GC) were performed on a Shimadzu GC-16A instrument using a 2 m column packed with silicone DC-200 or Carbowax 20 m. In GC experiments, n-decane was used as an internal standard. The identification and quantification of the products were done by GC using the response factors of standard samples. The ICP analyses were performed on an ICP-Spectrociros

CCD instrument. EPR spectra were recorded on polycrystalline samples with a Bruker Elexsys E500 spectrometer using the X-band (9.45 GHz) microwave frequency operating at 100 kHz. The measurements were performed at 4.2 K and a Cr(III) ($g = 1.9797$) in MgO sample was used for field calibration. The powder diffraction pattern of **1** was obtained using an X-ray powder diffractometer (XRD D5000 Siemens) with Cu Kα radiation. Measurements were made in a 2θ range of 5–40° at room temperature.

2.3. *Synthesis of [Co(mef)2(HIm)2(CH3OH)2] (1)*

Mefenamic acid (0.4 mM, 97 mg) was dissolved in methanol (15 ml) followed by addition of KOH (0.4 mM, 22 mg). After 1 h stirring, the solution was added slowly, and simultaneously, with a methanolic solution of imidazole (0.4 mM, 28 mg), to a methanolic solution (10 ml) of $CoCl_2 \cdot 6H_2O$ (0.2 mM, 48 mg) and stirred for 30 min. The solution was left for slow evaporation. Rose-colored crystals of **1** suitable for X-ray structure determination were deposited after ten days (yield 85%, 125.8 mg). m.p. 241–243 °C.

Anal. Calcd for $C_{38}H_{44}CoN_6O_6$ (MW = 739.72) C, 61.64; H, 5.90; N, 11.35%; found: C, 61.81; H, 5.70; N, 11.31%. IR: ν_{max}, cm^{-1}; ν(OH): 3670, $\nu_{asym}(CO_2)$: 1583 (vs); $\nu_{sym}(CO_2)$: 1385 (vs); $\Delta = \nu_{asym}(CO_2) - \nu_{sym}(CO_2)$: 198; ν(C=N): 1429; ν(C–N): 1065, 1094 cm^{-1} (KBr disk). UV–vis: λ/nm (log ε) as Nujol mull: 294, 381, 418, 557, 744; in DMSO: 301 (3.61), 384 (3.09), 430 (1.51), 563 (1.82), 757 (1.80). **1** is soluble in DMSO. Also, this complex is a non-electrolyte ($\Lambda_M = 6$ mho cm^2 M^{-1} in DMSO).

2.4. *Crystal structure determination*

Relevant details of data collection and structure solution are summarized in table 1. Crystals of **1** for X-ray crystallography were grown by slow evaporation of a methanol solution. An

Table 1. Crystallographic data for **1**.

Empirical formula	$C_{38}H_{44}CoN_6O_6$
Formula weight	739.72
T/K	297.1(6)
Crystal system	Triclinic
Space group	*P-1*
a/Å	7.5606(6)
b/Å	8.2515(5)
c/Å	15.2903(9)
α/°	104.433(5)
β/°	91.691(5)
γ/°	90.779(6)
V/Å^3	923.18(11)
Z	1
μ (mm^{-1})	0.52
D_{cal} /Mg m^{-3}	1.331
F(0 0 0)	389
Θ Range/°	3.3–25.4
Independent reflections	3373 [R(int) = 0.0259]
Data/restraints/parameters	3373/1/247
Goodness-of-fit on F^2	1.049
Final R indices	$R_1 = 0.0432$, $wR_2 = 0.1005$
R indices (all data)	$R_1 = 0.0558$, $wR_2 = 0.1085$
Largest difference peak and hole (e Å^{-3})	0.272, −0.237

Oxford Diffraction Xcalibur system was used to collect X-ray diffraction data. The crystal structures were solved by direct methods (Shelxt 2014) and refined by full matrix least squares using Shelxl 2014 within the Oscail package [37, 38]. Drawings were produced using ORTEX within the Oscail package. Non-hydrogen atoms were refined anisotropically. Hydrogens were in calculated positions using a riding model except for the hydrogen on N3 which was refined with a distance restraint of 0.89 Å.

2.5. *Catalytic reactions*

All reactions were carried out in a 25 ml glass reactor which was equipped with a reflux condenser. In a typical procedure, a mixture of alkene (0.5 mM), crystalline **1** as catalyst (0.01 mM) and *tert*-BuOOH (1.5 mM) in 1,2-dichloroethane, 1,2-DCE (2 ml), was prepared and heated under reflux. The reaction progress was monitored by GC. At the end of the reaction, the catalyst was filtered off and washed with CH_2Cl_2 (10 ml).

3. Results and discussion

3.1. *Synthesis and spectroscopic characterization*

The synthesis of **1** in high yield was achieved via the aerobic reaction of mefenamic acid (Hmef) and KOH with $CoCl_2{\cdot}6H_2O$ in the presence of imidazole (HIm) according to the equation:

$$\begin{aligned} &CoCl_2{\cdot}6H_2O + 2Hmef + 2KOH + 2HIm + 2CH_3OH \\ &\quad \rightarrow \left[Co(mef)_2(HIm)_2(CH_3OH)_2\right] + 2KCl + 8H_2O \end{aligned} \tag{1}$$

This complex is microcrystalline or powder-like and stable in atmospheric conditions. Complex **1** is insoluble in water and also in most common organic solvents, but is soluble in DMSO. The melting point of this complex is 241–243 °C. The elemental analysis confirms its stoichiometry.

In the IR spectrum, the observed absorption at 3670 cm^{-1} is attributed to ν(O–H) of coordinated methanol. The bands at 1661 and 1265 cm^{-1} attributed to ν_{asym}(C=O) and ν_{sym}(C=O) of the carboxylic moiety of Hmef, respectively, are shifted in IR spectra of **1** to 1583 and 1385 cm^{-1}. The difference Δ, [ν_{asym}(C=O) − ν_{sym}(C=O)], a useful tool for determining the coordination mode of the carboxylate, has a value of 198 cm^{-1} for **1** which is indicative of an asymmetrically monodentate binding mode for mefenamate [36, 39]. In the IR spectrum of imidazole ligand, strong bands at 1592 and 1482 cm^{-1} have been assigned to ν(C=C) and ν(C=N) of the imidazole ring. The very strong band at 1057 cm^{-1} and a medium band at 1084 cm^{-1} are assigned to imidazole C–N stretching vibrations. Upon coordination, HImd ν(C–N) and ν(C=N) are shifted to lower energies [40].

The UV–vis spectra of **1** have been recorded as Nujol mull and in DMSO solution and are similar, suggesting that **1** retains its structure in solution. In the visible region, three low-intensity bands are observed and can be assigned to d–d transitions. For local O_h symmetry, band I observed in 757 nm may be attributed to a $^4T_{1\ g}(F) \rightarrow {}^4T_{2\ g}$ transition, band

II at 563 nm to a $^4T_{2\ g}(F) \rightarrow {}^4A_{2\ g}$ transition, and band III at 430 nm to a $^4T_{1\ g}(F) \rightarrow {}^4T_{1\ g}(P)$ transition and are characteristic for distorted octahedral highspin Co^{2+} complexes. Furthermore, absorption assigned to charge transfer transition for the mefenamate ligand is at 384 nm [36].

3.2. *A description of the crystal structure of 1*

An ORTEX drawing of the asymmetric unit of **1** is shown in figure 1 and the full coordination sphere of **1** is shown in figure 2. Selected bond distances and angles are listed in table 2 and hydrogen bond details are in table 3. The complex is mononuclear and the monodentate deprotonated mefenamato ligand is coordinated to cobalt via carboxylate oxygen. The six-coordinate octahedral cobalt lies on an inversion center and is surrounded by two monodentate mefenamate ligands, two methanol molecules, and two imidazole ligands. The bond distances around cobalt are 2.0893(15) for Co–O1 to 2.1550(18) Å for Co–O3 and are within the normal range for cobalt(II) distances to oxygen and nitrogen [41]. The C1–O1 and C1–O2 distances of 1.254(3) and 1.267(3) Å would normally be expected for the non-coordinated oxygen to have the shortest carbon–oxygen bond with greatest amount of double bond character [41]. The unusual lengthening of the C1–O2 bond is probably due to hydrogen bonding. There are three hydrogen bonds of moderate strength and all involve O2 as an acceptor (figure 3 and table 3) [42]. The reasons for lengthening of the A–Y bond in an X–D–H···A–Y interaction have been discussed and is probably the involvement of O2 in three hydrogen bonds that is responsible for the lengthening observed here [43]. The hydrogen bonding generates a 1 d motif running parallel to the *b* axis (figure 3).

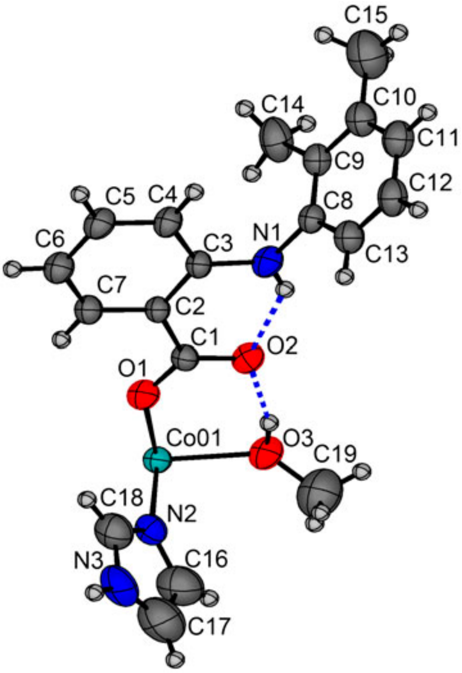

Figure 1. ORTEX (40% ellipsoids) diagram of the asymmetric unit of **1** with atom numbering scheme.

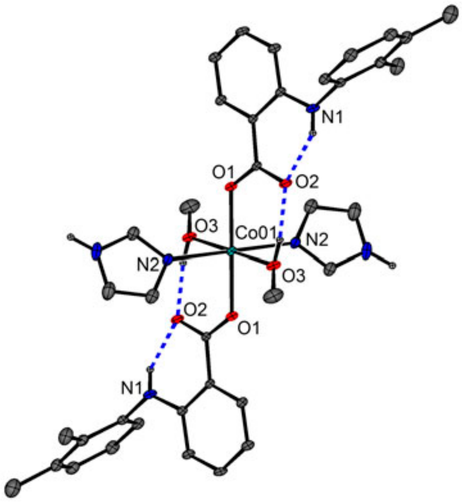

Figure 2. A drawing of the coordination sphere of **1** hydrogen atoms not involved in hydrogen bonding have been omitted for clarity.

Table 2. Selected bond distances (Å) and angles (°) for **1**.

Bond	Distance (Å)	Bond	Distance (Å)
Co(01)–O(1)	2.089(15)	Co(01)–O(3)	2.155(18)
Co(01)–N(2)	2.093(2)	O(2)–C(1)	1.267(3)
O(1)–C(1)	1.254(3)		
Angle	(°)	Angle	(°)
O(1)–Co(01)–N(2)	90.45(8)	O(1)–Co(01)–O(1)	180.0
N(2)–Co(01)–N(2)	180.00(5)	O(1)–Co(01)–O(3)	91.16(7)
O(3)–Co(01)–O(3)	180.0	N(2)–Co(01)–O(3)	92.90(8)
C(19)–O(3)–Co(01)	136.20(2)	C(1)–O(1)–Co(01)	129.67(16)

Symmetry transformations used to generate equivalent atoms: #1 –*x*, –*y* + 1, –*z*.

Table 3. Hydrogen bonds for **1** [Å and °].

D–H···A	d(D–H)	d(H···A)	d(D···A)	<(DHA)
N(1)–H(1N1)···O(2)	0.79(3)	2.04(3)	2.647(3)	133(2)
O(3)–H(1O3)···O(2)	0.86(3)	1.79(4)	2.615(2)	162(3)
N(3)–H(1N3)···O(2)#2	0.858(18)	2.09(2)	2.873(3)	151(3)

Symmetry transformations used to generate equivalent atoms: #1 –*x*, –*y* + 1, –*z*; #2 *x*, *y*–1, *z*.

A comparison of the cobalt–oxygen bond distances in **1** with those in other Co-mefenamato complexes are presented in table 4. The $(\text{Co–O})_{\text{mef}}$ bond length of **1** is 2.089 Å in comparison with 2.060 and 2.063 in $[\text{Co(mef)}_2(\text{MeOH})_4]\cdot 2\text{MeOH}$ and $[\text{Co(mef)}_2(\text{bipy})(\text{MeOH})_2]$, respectively.

The bulk powder X-ray diffraction pattern (PXRD) of **1** and a pattern simulated using the atom coordinates of the crystal structure are a close match (figure 4). This demonstrates that the crystal structure is representative of the bulk sample.

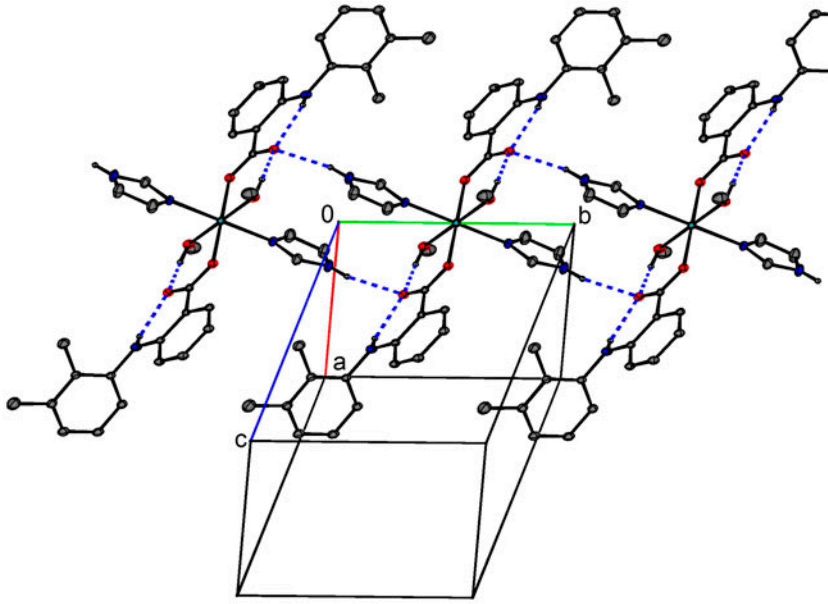

Figure 3. 1-d hydrogen bonding motif running along b. Hydrogen atoms not involved in hydrogen bonding have been omitted for clarity.

Table 4. Comparison of cobalt–oxygen bond distances (Å) in various cobalt(II) derivatives.

Compound	Geometry	Distance (Co–O)$_{(mef)}$ (Å)	Ref.
[Co(mef)$_2$(MeOH)$_4$]·2MeOH	Octahedral	2.060(2)	[36]
[Co(mef)$_2$(bipy)(MeOH)$_2$]	Octahedral	2.063(2)	[36]
[Co(mef)$_2$(HIm)$_2$(CH$_3$OH)$_2$	Octahedral	2.089(15)	This work

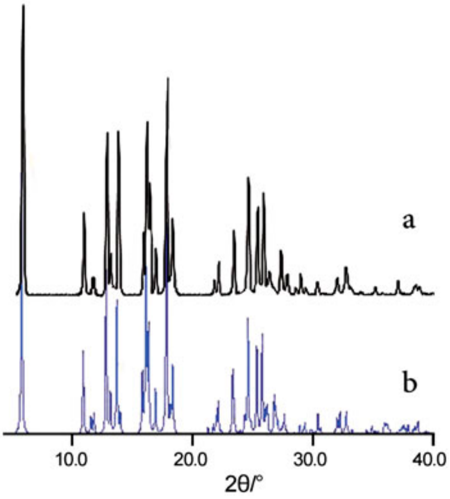

Figure 4. Powder X-ray diffraction (PXRD) patterns of **1** (a) **1** simulation based on the single-crystal structure, (b) the as-synthesized **1**.

3.3. *EPR spectra*

The EPR spectrum of **1** was obtained using polycrystalline samples at 4.2 K (see figure 5). Due to large anisotropy of cobalt(II) complexes, the intermolecular exchange interactions do not cause exchange narrowing and the signals of individual molecules are resolved [44]. However, the high- and low-field attributes are very broad, as a result of unresolved metal hyperfine coupling. In comparison, six-coordinate [(*t*Bu-pyp)$CoCl_2$] (pyp=pyridinophane) [45], $[Co(mef)_2(bipy)(MeOH)_2]$ (bipy = 2,2′-bipyridine), and ($[Co(mef)_2(MeOH)_4]\cdot 2MeOH$ [36] have very broad X-band EPR spectra in the range $g = 2–6$, characteristic of high-spin ($S = 3/2$) cobalt(II) species. As a result, the g-values $g_1 = 2.2$, $g_2 = 2.4$, and $g_3 = 6.3$ for **1** are within the range reported for mononuclear highspin Co(II) complexes ($S = 3/2$). The large variation of the g-values is expected in consideration of the high sensitivity of the g-values of Co(II) with regard to any weak distortion of the ligand field.

3.4. *Catalytic behavior*

3.4.1. Application as epoxidation catalysts. Optimum conditions were established from catalytic runs using cyclohexene as substrate, **1** as catalyst, and *tert*-BuOOH, TBHP, as oxidant in 1,2-DCE solution (tables 5 and 6). The optimum conditions for the oxidation of cyclohexene by this catalytic system was with catalyst, oxidant, and substrate in a molar ratio of 1:150:50 as established by runs 3 and 4. Under these conditions, cyclohexene oxide was produced with 100% selectivity. Different solvents were also tested in the oxidation of cyclohexene with TBHP and 1,2-dichloroethane gave the best conversion (table 7, run 1).

The effect of different oxidants was tested using H_2O_2, $NaIO_4$, and TBHP. The results showed that TBHP was the best oxygen source (table 8, run 3). The reaction temperature was also optimized by repeating the reaction in various temperatures. At room temperature (25 °C), the product yields were low and increasing the reaction temperature to 75 °C (refluxing 1,2-DCE) gave the best conversion (table 9, run 4). In 1,2-dichloroethane in the absence of catalyst, the amount of epoxide formed was less than 10%. Complex **1** was applied as an epoxidation catalyst, under conditions optimized for cyclohexene, to seven

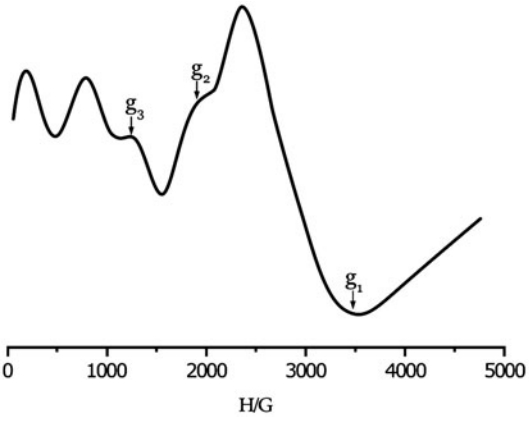

Figure 5. EPR spectra of polycrystalline samples of **1** recorded at 4.2 K and 9 GHz.

Table 5. Optimization of oxidant amount in the oxidation of cyclohexene catalyzed by **1**[a].

Run	TBHP (mM)	Conversion (%)[a]
1	0.5	29
2	1.0	73
3	1.5	100
4	2.0	100

[a]Reaction conditions: alkene (0.5 mM), catalyst (0.01 mM), 1,2-DCE (2 ml), *T* = 75 °C, *t* = 4 h.

Table 6. Optimization of catalyst amount in the oxidation of cyclohexene with TBHP catalyzed by **1**[a].

Run	Catalyst (mM)	Conversion (%)[a]
1	0.002	19
2	0.005	38
3	0.007	72
4	0.010	100

[a]Reaction conditions: alkene (0.5 mM), TBHP (1.5 mM), 1,2-DCE (2 ml), *T* = 75 °C, *t* = 4 h.

Table 7. Effect of solvent on the oxidation of cyclohexene catalyzed by **1**[a].

Run	Solvent	Conversion (%)[a]	Form of catalysis
1	1,2-dichloroethane	100	Heterogeneous
2	CH_3OH	5	Heterogeneous
3	CH_2Cl_2	53	Heterogeneous
4	CH_3COCH_3	7	Heterogeneous
5	CCl_4	18	Heterogeneous
6	$CHCl_3$	67	Heterogeneous

[a]Reaction conditions: alkene (0.5 mM), TBHP (1.5 mM), catalyst (0.01 mM), solvent (2 ml), *T* = 75 °C, *t* = 4 h.

Table 8. Effect of different oxidants on the oxidation of cyclohexene catalyzed by **1**[a].

Run	Oxidant	Conversion (%)	Time (h)
1	H_2O_2[a]	10	4
2	$NaIO_4$[b]	20	4
3	TBHP[c]	100	4
4	No oxidant	5	4

[a]Reaction conditions: biphasic system: alkene (0.5 mM), H_2O_2 (1.5 mM), catalyst (0.01 mM), 1,2-dichloroethane (2 ml) under reflux conditions (*T* = 75 °C).
[b]biphasic system: alkene (0.5 mM), $NaIO_4$ (1.5 mM), catalyst (0.01 mM), 1,2-dichloroethane (1.5 ml)+H_2O (0.5 ml) under reflux conditions (*T* = 75 °C).
[c]alkene (0.5 mM), TBHP (1.5 mM), catalyst (0.01 mM), 1,2-dichloroethane (2 ml) under reflux conditions (*T* = 75 °C).

other alkenes. The results are shown in table 10, where TOF is turnover frequency. The complex showed potential and selectivity as catalyst in the epoxidation of alkenes at 75 °C in the presence of TBHP as oxidant. Oxidation of cyclooctene like cyclohexene went with 100% yield and 100% selectivity while in the case of styrene, the major product was

Table 9. The effect of temperature on the oxidation of cyclohexene catalyzed by **1**[a].

Run	Temperature (°C)	Conversion (%)[a]
1	25	6
2	40	15
3	60	31
4	75 (reflux)	100

[a] Reaction conditions: alkene (0.5 mM), TBHP (1.5 mM), catalyst (0.01 mM), 1,2-dichloroethane (2 ml), $t = 4$ h.

Table 10. Oxidation of alkenes with TBHP catalyzed by **1**[a].

Entry	Alkene	Product[a]	Conversion (%)[b]	Selectivity (%)	TBHP efficiency (%)	Time (h)	TOF (h^{-1})
1	Cyclohexene	Cyclohexene oxide	100	100	71	4	8.33
2	1-methylcyclohexene	1-methylcyclohexene oxide	100	100	73	4	8.33
3	Cyclooctene	Cyclooctane oxide	100	100	67	4	8.33
4	Limonene	Limonene oxide	90	95	41	4	4.88
5	Dihydronaphthalene	Exo-epoxide	92	98	45	5	4.83
6	Styrene	1) Styrene oxide 2) Benzaldehyde	67	1) 41 2) 59	44	4	4.92
7	1-heptene	1-heptene oxide	71	100	48	4	5.51
8	1-octene	1-octene oxide	67	100	39	4	4.81

[a] Reaction conditions: alkene (0.5 mM), TBHP (1.5 mM), catalyst (0.01 mM), 1,2-dichloroethane (2 ml), $T = 75$ °C, $t = 4$ h. The identification and quantification of products are done by GC.

[b] GLC yield based on starting alkene.

[c] The ratio of given product per consumed alkene.

benzaldehyde. The non-activated 1-octene and 1-heptene converted into the corresponding epoxides with 67–71% yield and 100% selectivity.

The consumption of TBHP was determined iodometrically after each catalytic reaction. The efficiency of TBHP was calculated according to reported procedure [46, 47] as follows:

$$\text{TBHP efficiency } (\%) = (\text{mM of products/mM of TBHP consumed}) \times 100$$

As shown in table 11, the performance of the catalyst **1** towards the cyclohexene oxidation is compared to some other catalysts. Based on this consideration, oxidation of cyclohexene with 100% yield and 100% selectivity is comparable with other reported catalysts for which the conversion is lower than 100%.

The catalysts of $(Himi)_4[(imi)_2(Mo_8O_{26})]\cdot H_2O$ (**2**), $(H_2bbi)_2[Mo_8O_{26}]$ (**3**), and $(H_2bbi)[(Hbbi)_2(Mo_8O_{26})]\cdot H_2O$ (**4**) {H_2bbi = 1,1′-(1,4-butanediyl)bis(imidazolium)} have been used in the epoxidation of olefins with TBHP as the oxidant, that catalyst **2** showed much higher catalytic activity than catalyst **3** or **4** [48]. This property has been attributed to the presence of coordinated imidazole ligands in this compound. Coordination of electron-donating molecules such as imidazole may enhance the electropositivity of the metal center, thus resulting in the improvement of its ability to attract or capture nucleophilic groups, which leads to the improvement of the epoxidation activity of the catalyst [48, 49]. From this point of view, it is proposed that **1** shows effective catalyst in the epoxidation of olefins due to the presence of heterocyclic imidazole as ligand.

Table 11. Catalytic activity towards cyclohexene oxidation of some previously reported catalysts.

Catalyst	Rxn time (min.)	Rxn temp. (°C)	Oxidant	Conv. (%)	Amount of catalyst (mM)	Ref.
$[MoO_2L^1(CH_3OH)]\cdot CH_3OH$[a]	74.5	R.T.[h]	H_2O_2	95	0.094×10^{-2}	[50]
$[MoO_2L^2(CH_3OH)]$[b]	74.5	R.T.[h]	H_2O_2	97	0.094×10^{-2}	[50]
$[WO(O_2)L(CH_3OH)]$[c]	74.5	R.T.[h]	H_2O_2	93	0.094×10^{-2}	[51]
$[VOL^1L]$[d]	60	80	TBHP	87.2	0.032	[52]
$[VOL^2L]$[e]	60	80	TBHP	90.3	0.032	[52]
Metallocorrole[f]	180	0	TBHP	39	0.025	[53]
Co(II) calix[4]pyrrole	1440	R.T.[h]	2-ethyl-butyraldehyde/O_2	86	0.050	[54]
$[Co_2(L)_2(\mu_{1,1}\text{–}N_3)_2(N_3)_2]$	<<60	0	m-CPBA	99	0.020	[21]
$[\{Co^{II}Cl_3\}(tptz$[g]$)\{Co^{II}Cl(H_2O)\}]\cdot 0.25H_2O$	480	80	TBHP	54	0.084	[55]
$[Co(mef)_2(HIm)_2(CH_3OH)_2]$	240	75	TBHP	100	0.010	This work

[a] L^1: dianion of N′-(3-bromo-2-hydroxybenzylidene)-4-hydroxybenzohydrazide.
[b] L^2: dianion of N′-(2-hydroxybenzylidene)-2-hydroxy-3-methylbenzohydrazide.
[c] L: dianion of salicylidene benzoyl hydrazine.
[d] L^1: dianion of N′-(3,5-dibromo-2-hydroxybenzylidene)-4methoxybenzohydrazide, L: benzohydroxamate.
[e] L^2: dianion of N′-(3,5-dibromo-2-hydroxybenzylidene) nicotinohydrazide, L: benzohydroxamate.
[f] meso-tris(pentafluorophenyl)-corrolatomanganese(III) or meso-tris(pentafluorophenyl)-corrolatoiron(IV)chloride.
[g] tptz = 2,4,6-tris(2-pyridyl)-1,3,5-triazine.
[h] R.T.= Room temperature.

3.4.2. Blank experiments. Cyclohexene epoxidation experiments performed without a catalyst (using the same conditions as the catalytic runs) gave negligible conversion after 4 h and the selectivity for epoxide was close to zero. After 24 h of reaction, the conversion was less than 7% and the selectivity for epoxide was less than 10%.

3.4.3. Catalyst reuse and stability. To evaluate long-term stability and reusability of **1**, epoxidation of cyclohexene was chosen as a model reaction and recycling experiments were performed with a single sample of the catalyst. Following every experiment, the catalyst was removed by simple filtration, rinsed with CH_2Cl_2, dried, and recycled. After reusing catalyst four consecutive times, the conversion was 90% (table 12). No cobalt was detected in the filtrates as determined by atomic absorption spectroscopy, AAS, after each reaction at the detection limit of AAS. Therefore, we decided to measure the amount of Co leached by ICP. This method has a lower detection limit than AAS of 0.1 μg/L and this showed 1.1% of cobalt (based on the amount of Co loading before the specific run) in the first run. Also,

Table 12. Investigation of catalyst reusability and the amount of Co leached in the epoxidation of cyclohexene with TBHP[a].

Run	Conversion (%)	Amount of Co leached (%)[b]
1	100	1.1
2	90	0
3	90	0
4	90	0
5	90	0

[a] Reaction conditions: cyclooctene (0.5 mM), TBHP (1.5 mM).
[b] Determined by ICP.

the catalytic behavior of the separated liquid was tested by addition of fresh alkene and TBHP to the filtrates following each run. The results from these experiments were the same as the blank experiments.

4. Conclusion

The synthesis and characterization of $[Co(mef)_2(HIm)_2(CH_3OH)_2]$ (**1**) with the mefenamic acid anion and imidazole ligands have been achieved. In this complex, the mefenamate is bound to cobalt(II) via a carboxylate oxygen. This complex was characterized structurally and it has a distorted octahedral geometry around cobalt. Complex **1** exhibits good catalytic activity in the epoxidation of a range of alkenes including non-activated terminal alkenes. Its ready preparation, reaction under mild reaction conditions and moderate to high conversion with very high selectivities makes this a very useful catalytic system for the epoxidation of alkenes. The catalyst is reusable and this heterogeneous catalyst can be effortlessly separated and recycled.

Acknowledgements

We are grateful for the financial support from the Department of Chemistry, Isfahan University of Technology (IUT). Also, the authors would like to thank the Raha Pharmacological Company for providing us with the required mefenamic acid.

References

[1] R.E. Parker, N.S. Isaacs. *Chem. Rev.*, **59**, 737 (1959).
[2] N. Gharah, S. Chakraborty, A.K. Mukherjee, R. Bhattacharyya. *Chem. Commun.*, **22**, 2630, (2004).
[3] M. Herbert, E. Alvarez, D.J. Cole-Hamilton, F. Montilla, A. Galindo. *Chem. Commun.*, **46**, 5933, (2010).
[4] C.J. Thibodeaux, W.C. Chang, H.W. Liu. *Chem. Rev.*, **112**, 1681 (2012).
[5] A.K. Yudin. *Aziridines and Epoxides in Organic Synthesis*, Wiley-VCH, Weinheim (2006).
[6] G. Sienel, R. Rieth, K.T. Rowbottom. *Epoxides*, VCH Publishers, New York, NY (1985).
[7] N. Grover, F.E. Kühn. *Curr. Org. Chem.*, **16**, 16 (2012).
[8] M. Wu, C. Miao, S. Wang, X. Hu, C. Xia, F.E. Kühn, W. Sun. *Adv. Synth. Catal.*, **353**, 3014 (2011).
[9] D. Betz, P. Altmann, M. Cokoja, W.A. Herrmann, F.E. Kühn. *Coord. Chem. Rev.*, **255**, 1518 (2011).
[10] D. Betz, A. Raith, M. Cokoja, F.E. Kühn. *ChemSusChem*, **3**, 559 (2010).
[11] K.R. Jain, F.E. Kühn. *Dalton Trans.*, 2221, (2008).
[12] F.E. Kühn, A.M. Santos, M. Abrantes. *Chem. Rev.*, **106**, 2455 (2006).
[13] Q.H. Xia, H.Q. Ge, C.P. Ye, Z.M. Liu, K.X. Su. *Chem Rev.*, **105**, 1603 (2005).
[14] D.E. Hamilton, R.S. Drago, A. Zombeck. *J. Am. Chem. Soc.*, **109**, 374 (1987).
[15] B. Rhodes, S. Rowling, P. Tidswell, S. Woodward, S.M. Brown. *J. Mol. Catal. A: Chem.*, **116**, 375 (1997).
[16] R.I. Kureshy, N.H. Khan, S.H.R. Abdi, A.K. Bhatt, P. Iyer. *J. Mol. Catal. A: Chem.*, **121**, 25 (1997).
[17] P. Buranaprasertsuk, Y. Tangsakol, W. Chavasiri. *Catal. Commun.*, **8**, 310 (2007).
[18] A. Zhang, L. Li, J. Li, Y. Zhang, S. Gao. *Catal. Commun.*, **12**, 1183 (2011).
[19] M.M. Reddy, T. Punniyawurthy, J. Iqbal. *Tetrahedron Lett.*, **36**, 159 (1995).
[20] J. Estrada, I. Fernandez, J. Pedro, X. Ottenwaelder, R. Ruiz, Y. Journaux. *Tetrahedron Lett.*, **38**, 2377 (1997).
[21] A. Ray, G.M. Rosair, G. Pilet, B. Dede, C.J. Gómez-García, S. Signorella, S. Bellú, S. Mitra. *Inorg. Chim. Acta*, **375**, 20 (2011).
[22] T. Joseph, D.P. Sawant, C.S. Gopinath, S.B. Halligudi. *J. Mol. Catal. A: Chem.*, **184**, 289 (2002).
[23] P. Oliverira, A.M. Ramos, I. Fonseca, A. Botelho do Rego, J. Vital. *Catal. Today*, **103**, 67 (2005).
[24] T. Toshihiro, H. Eiichiro, Y. Kiyotaka, T. Mukaiyama. *Chem. Lett.*, **10**, 2077 (1992).
[25] R. Chakrabarty, B.K. Das. *J. Mol. Catal. A: Chem.*, **223**, 39 (2002).
[26] E.K. Beloglazkina, A.G. Majouga, R.B. Romashkinaand, N.V. Zyk. *Tetrahedron Lett.*, **47**, 2957 (2006).

[27] D. Saha, T. Maity, R. Bera, S. Koner. *Polyhedron*, **56**, 230 (2013).
[28] S. Bhunia, S. Jana, D. Saha, B. Dutta, S. Koner. *Catal. Sci. Technol.*, **4**, 1820 (2014).
[29] Q. Tang, Q. Zhang, H. Wu, Y. Wang. *J. Catal.*, **230**, 384 (2005).
[30] S.K. Choi, H.J. Lee, H. Kim, W. Nam. *Bull. Korean Chem. Soc.*, **23**, 1039 (2002).
[31] K.J. O'Connor, S.J. Wey, C.J. Burrows. *Tetrahedron Lett.*, **33**, 1001 (1992).
[32] V.B. Sharma, S.L. Jain, B. Sain. *J. Mol. Catal. A: Chem.*, **227**, 47 (2005).
[33] T. Punniyamurthy, S. Velusamy, J. Iqbal. *Chem. Rev.*, **105**, 2329 (2005).
[34] D. Kovala-Demertzi. *J. Organomet. Chem.*, **691**, 1767 (2006).
[35] D. Kovala-Demertzi, D. Hadjipavlou-Litina, M. Staninska, A. Primikiri, C. Kotoglou, M.A. Demertzis. *J. Enzyme Inhib. Med. Chem.*, **24**, 742 (2009).
[36] F. Dimiza, A.N. Papadopoulos, V. Tangoulis, V. Psycharis, C.P. Raptopoulou, D.P. Kessissoglou, G. Psomas. *Dalton Trans.*, 4517 (2010).
[37] G. Sheldrick. *Acta Crystallogr., Sect. A*, **64**, 112 (2008).
[38] P. McArdle, K. Gilligan, D. Cunningham, R. Dark, M. Mahon. *CrystEngComm*, **6**, 303 (2004).
[39] K. Nakamoto. *Infrared and Raman Spectra of Inorganic and Coordination Compounds, Part B: Applications in Coordination, Organometallic, and Bioinorganic Chemistry*, 6th Edn., John Wiley & Sons, New York (2009).
[40] B. Morzyk-Ociepa, E.R. Sokołowska, D. Michalska. *J. Mol. Struct.*, **1028**, 49 (2012).
[41] D. Li, G. Zhong. *Sci World J*, **2014**, 1 (2014).
[42] T. Steiner. *Angew. Chem. Int. Ed.*, **41**, 48 (2002).
[43] F. Mohri. *J. Mol. Struct. Theochem*, **770**, 179 (2006).
[44] A. Bencini, C. Benelli, D. Gatteschi, C. Zanchini. *Inorg. Chem.*, **19**, 3027 (1980).
[45] T. Martijn Kooistra, K.F.W. Hekking, Q. Knijnenburg, B. DeBruin, P.H.M. Budzelaar, R. Gelder, J.M.M. Smits, A.W. Gal. *Eur. J. Inorg. Chem.*, **2011**, 648 (2003).
[46] D. Kishore, A.E. Rodrigues. *Catal. Commun.*, **8**, 1156 (2007).
[47] S. Khare, R. Chokhare. *J. Mol. Catal. A: Chem.*, **344**, 83 (2011).
[48] J. Du, J. Yu, J. Tang, J. Wang, W. Zhang, W.R. Thiel, M. Jia. *Eur. J. Inorg. Chem.*, **2011**, 2361, (2011).
[49] J.-Y. Liu, X.-F. Li, Y.-Z. Li, W.-B. Chang, A.-J. Huang. *J. Mol. Catal. A: Chem.*, **187**, 163 (2002).
[50] X.-Q. He. *J. Coord. Chem.*, **66**, 966 (2013).
[51] M. Amini, M. Bagherzadeh, B. Eftekhari-Sis, A. Ellern, J. Keith Woo. *J. Coord. Chem.*, **66**, 1897 (2013).
[52] A.-M. Li. *J. Coord. Chem.*, **67**, 2076 (2014).
[53] S. Bosea, A. Pariyara, A. Narayan Biswas, P. Bandyopadhyay. *J. Mol. Catal. A: Chem*, **378**, 179 (2013).
[54] P. Buranaprasertsuk, Y. Tangsakol, W. Chavasiri. *Catal. Commun.*, **8**, 310 (2007).
[55] M. Maghami, F. Farzaneh, J. Simpson, A. Moazeni. *Polyhedron*, **73**, 22 (2014).